

Autogenous shrinkage of ultra high performance concrete considering early age coefficient of thermal expansion

Jung-Jun Park^{1a}, Doo-Yeol Yoo^{2b}, Sung-Wook Kim^{1c} and Young-Soo Yoon^{*2}

¹Structural Engineering Research Division, Korea Institute of Construction Technology, Korea

²School of Civil, Environmental and Architectural Engineering, Korea University, Korea

(Received March 7, 2013, Revised December 12, 2013, Accepted February 1, 2014)

Abstract. The recently developed Ultra High Performance Concrete (UHPC) displays outstanding compressive strength and ductility but is also subjected to very large autogenous shrinkage. In addition, the use of forms and reinforcement to confine this autogenous shrinkage increases the risk of shrinkage cracking. Accordingly, this study adopts a combination of shrinkage reducing admixture and expansive admixture as a solution to reduce the shrinkage of UHPC and estimates its appropriateness by evaluating the compressive and flexural strengths as well as the autogenous shrinkage according to the age. Moreover, the coefficient of thermal expansion known to experience sudden variations at early age is measured in order to evaluate exactly the autogenous shrinkage and the thermal expansion is compensated considering these measurements. The experimental results show that the compressive and flexural strengths decreased slightly at early age when mixing 7.5% of expansive admixture and 1% of shrinkage reducing admixture but that this decrease becomes insignificant after 7 days. The use of expansive admixture tended to premature the setting of UHPC and the start of sudden increase of autogenous shrinkage. Finally, the combined use of shrinkage reducing admixture and expansive admixture appeared to reduce effectively the autogenous shrinkage by about 47% at 15 days.

Keywords: ultra high performance concrete; coefficient of thermal expansion; autogenous shrinkage; setting properties; shrinkage reducing admixture; expansive admixture

1. Introduction

Concrete is the most commonly used construction material owing to its remarkable economic efficiency as well as its outstanding mechanical performance and durability. However, concrete is also accompanied by several problems such as its brittleness and the low strength developed in comparison to its weight. In order to overcome such limitations, Ultra High Performance Concrete (UHPC) achieving both ultra high strength and high toughness has been developed recently (Kamen *et al.* 2008, Kim *et al.* 2008).

UHPC is characterized by a very low water-to-binder ratio (W/B) and does not use coarse

*Corresponding author, Professor, E-mail: ysyoon@korea.ac.kr

^aSenior Researcher, E-mail: jjpark@kict.re.kr

^bPh.D. Candidate, E-mail: dooyoul@korea.ac.kr

^cResearch Fellow, E-mail: swkim@kict.re.kr

Table 1 Properties of steel fiber

Type of fiber	Density (g/cm ³)	Tensile strength (MPa)	Length of fiber (mm)	Shape factor (l_f/d_f) (mm/mm)
Straight fiber	7.8	2,500	13	65

Where, l_f = length of fiber, d_f = diameter of fiber

Table 2 Mix proportions of UHPC (ratio in weight)

	W/B	Cement	SF	Filler	Sand	Superplasticizer (SP)	Steel fiber	SRA	EA
Mix A	0.2	1	0.25	0.30	1.10	0.012	$V_f = 2\%$	-	-
Mix B								0.01	0.075

Where, V_f = volume fraction of fiber, SRA = shrinkage reducing admixture, EA = expansive admixture

aggregates, which induce extremely large autogenous shrinkage at early age. According to the results of Koh *et al.* (2011), UHPC experiences a final autogenous shrinkage strain of about 800 $\mu\epsilon$. Moreover, Yoo *et al.* (2011) reported that Ultra High Strength Concrete (UHSC) with W/B less than 20% also undergoes an autogenous shrinkage strain of approximately 800 $\mu\epsilon$ at 60 days. The confinement of such shrinkage through the use of forms and reinforcing bars will increase substantially the risk of excessive residual stresses and shrinkage cracking. Therefore, the exact understanding of the shrinkage behavior and studies on solutions to reduce shrinkage should be imperatively undertaken for further application of UHPC to real structures.

Among the methods deployed to reduce the shrinkage of concrete, studies are being performed on the inclusion of a combination of expansive admixture (EA) and shrinkage reducing admixture (SRA) (Park *et al.* 2013a, Maltese *et al.* 2005). In particular, based on previous study (Park *et al.* 2014), the combination of SRA and EA are more effective in reducing the restrained shrinkage strains than the mixture with EA or SRA alone. The mechanisms of reducing shrinkage from EA and SRA are as follows; EA expands the volume by favoring the hydration owing to its content in C₄A₃S clinker which generates large quantities of ettringite at early age, and SRA reduces shrinkage by decreasing the surface tension of water in the pores of the cement paste.

Meanwhile, the autogenous shrinkage is defined as the total strain from which the drying shrinkage and thermal strain are discarded. Here, the thermal strain is obtained by multiplying the internal thermal variation of concrete by the coefficient of thermal expansion (CTE). Former research reported that the CTE varies with the age of concrete (Loukili *et al.* 2000), and tends to exhibit large values at early age. Therefore, thermal compensation should be conducted by reflecting the varying CTE of concrete with respect to the age in order to achieve exact measurement of the autogenous shrinkage.

This study measured the compressive and flexural strength with respect to the age to evaluate the effects of the admixing of EA and SRA on the mechanical properties of UHPC. In addition, autogenous shrinkage tests were performed considering the measurements of the CTE with the age and the effects of EA and SRA on the reduction of the autogenous shrinkage of UHPC were evaluated.

2. Experiment

2.1 Materials and mix proportions

The tests adopted Portland cement of type 1, fine aggregates with grain size smaller than 0.5 mm, filler with mean grain size of $2\mu\text{m}$ including 98% of SiO_2 , silica fume (SF) produced in Norway, CSA EA from Japan, and glycol based SRA from Germany. The chemical composition of the materials involved in the mixes was identical to that of our previous study (Park *et al.* 2013a). Moreover, straight high strength steel fibers were incorporated at a ratio of 2% of the whole volume to enhance the toughness. The characteristics of the steel fibers are listed in Table 1. Table 2 presents the mix proportions adopted for the shrinkage test. Mix A and Mix B correspond respectively to the mixes without and with EA and SRA.

2.2 Compressive and flexural strength

The compressive strength was measured according to the age using a Universal Testing Machine (UTM) with capacity of 3000 kN on a series of three cylinders $\phi 100 \times 200\text{mm}$ fabricated

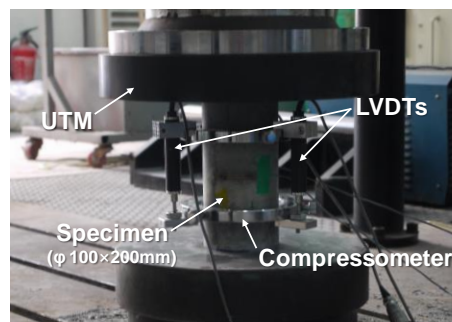


Fig. 1 Compression test (ASTM C 39)

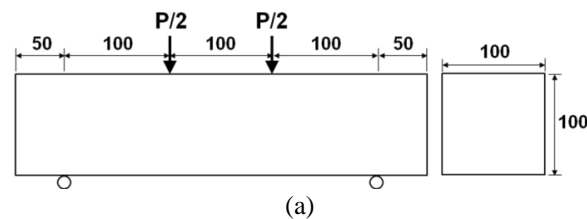


Fig. 2 4-point loading flexural test (ASTM C 1609); (a) geometry of specimen, (b) test setup

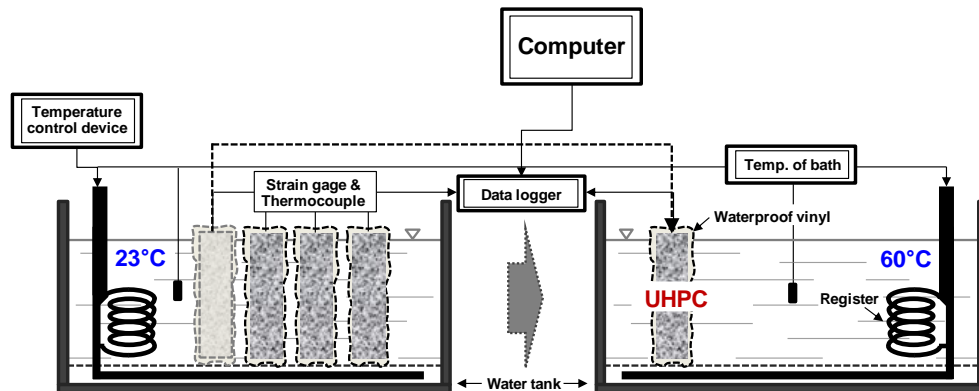


Fig. 3 Schematic description of the experimental system for measurement of CTE

in compliance with ASTM C 39 (2009) (Fig. 1). The flexural strength was measured through 4-point loading flexural test using $100 \times 100 \times 400$ mm specimens in similar to ASTM C 1609 (2006) as shown in Fig. 2. Here also, the flexural test was performed on a series of three prisms according to the age identically to the compressive strength test and the corresponding mean values are used.

2.3 Penetration resistance

Penetration resistance test was carried out in compliance with ASTM C 403 (2008) to evaluate the setting characteristics of UHPC. According to the research of Yoo *et al.* (2013), UHPC tends to undergo sudden drying even when its surface is exposed for a short time due to its low W/B. This phenomenon appears through the premature occurrence of early and final settings. Following, liquid paraffin oil was applied on the surface of concrete to conduct the setting tests. A plastic container with dimensions of $\phi 150 \times 160$ mm was used as mold. Placing was done to place the surface of mortar at a distance of 10 mm below the top of the container so as to enable the application of liquid paraffin oil on the surface of mortar. The tests were performed in a constant temperature and humidity chamber at temperature of $23 \pm 1^\circ\text{C}$ and humidity of $60 \pm 5\%$.

2.4 Coefficient of thermal expansion (CTE)

The CTE was measured as follows. First, two water tanks at different temperatures (23°C and 60°C) were prepared. It should be noted that the thermal expansion of concrete appears in the form of volumetric expansion. This means that measurement error may be introduced by any confinement like the form. Following, the tests were executed by stripping off the forms after final setting. Moreover, since the shrinkage and expansion deformations differ according to the geometry of the specimen, the CTE was measured using specimens having an identical size with that of the autogenous shrinkage specimen. After stripping of the forms, the specimens were disposed in the water tank at 23°C and, the temperature and strain were measured using a concrete embedded gage with nearly zero stiffness and a thermocouple. Then, the specimens were moved in the water tank at 60°C at intervals of 1 to 2 h to measure the increased temperature and strain. Since this test procedure increased suddenly the temperature of concrete, no need was to consider equivalent age. The details of the test are illustrated in Fig. 3.

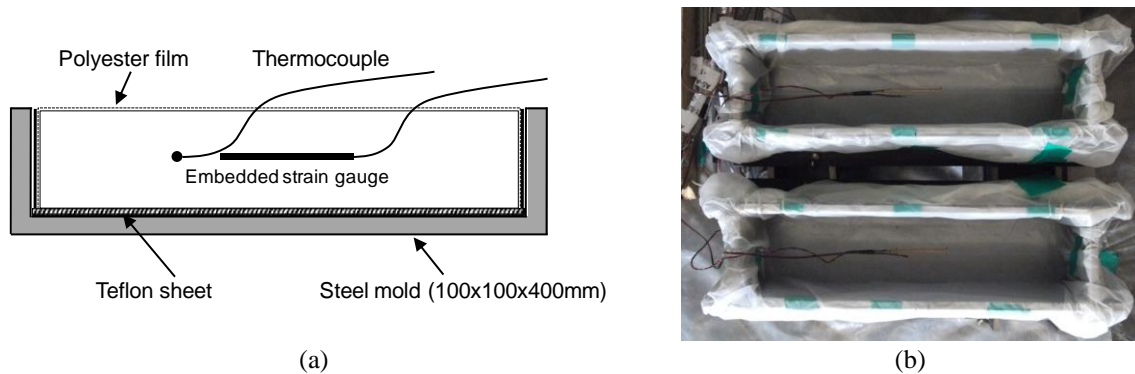


Fig. 4 Autogenous shrinkage measurement; (a) schematic description, (b) test setup

2.5 Autogenous shrinkage

The autogenous shrinkage was tested by a method similar to that proposed by the technical committee on autogenous shrinkage at Japan Concrete Institute (JCI) (1999) (Fig. 4). A dumbbell-shape embedded gage having nearly zero stiffness (Yoo *et al.*, 2014) and a thermocouple were installed and fixed at the center of the specimen, and then concrete was placed in the prismatic mold with dimensions of 100×100×400 mm, as shown in Fig. 4(b). A teflon sheet was disposed in the mold to remove the shrinkage confining force generated by the friction between the mold and concrete. A polyester film was also applied at the surface of concrete to prevent eventual evaporation or absorption of moisture. The mold was stripped off 24 h after placing of concrete. All the exposed surfaces were sealed by aluminum tape to prevent any volumetric reduction due to the evaporation after stripping. The tests were performed in a constant temperature and humidity chamber at temperature of 23±1 °C and humidity of 60±5%.

3. Results and discussion

3.1 Compressive and flexural strength

Fig. 5 plots the mean values of the compressive and flexural strengths of UHPC according to the age. The compressive and flexural strengths showed slight reduction at early age due to the admixing of EA and SRA but the difference between Mix A and Mix B practically disappeared after 7 days. At 28 days, the compressive strength was approximately 152 MPa for both mixes and the flexural strength reached 34 MPa and 33 MPa for Mix A and Mix B, respectively. According to Park *et al.* (2013a), the prediction formulae for the compressive and flexural strengths can be expressed as Eqs. (1) and (2).

$$f_c = f_{28} \cdot \exp\left(\frac{a}{b-t}\right) \quad (1)$$

$$f_{ft} = f_{ft,28} \cdot \exp\left(\frac{c}{d-t}\right) \quad (2)$$

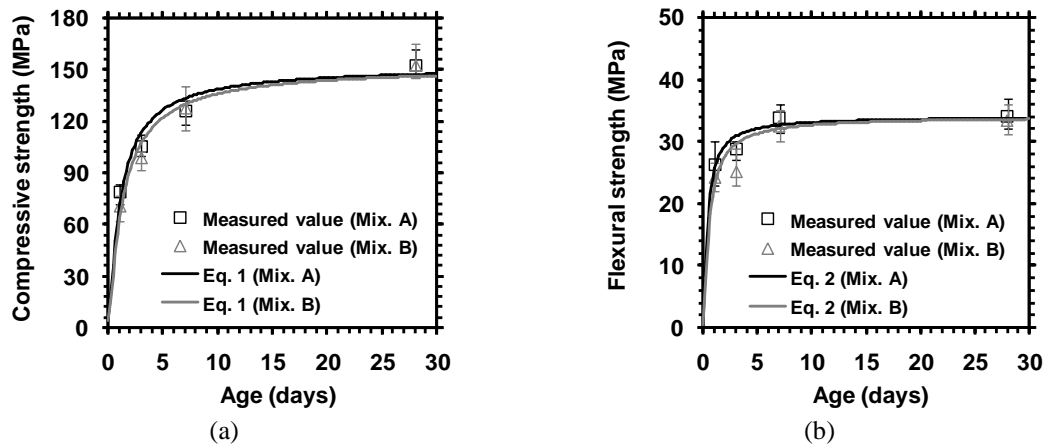


Fig. 5 Comparison of predicted values and experimental results; (a) compressive strength, (b) flexural strength

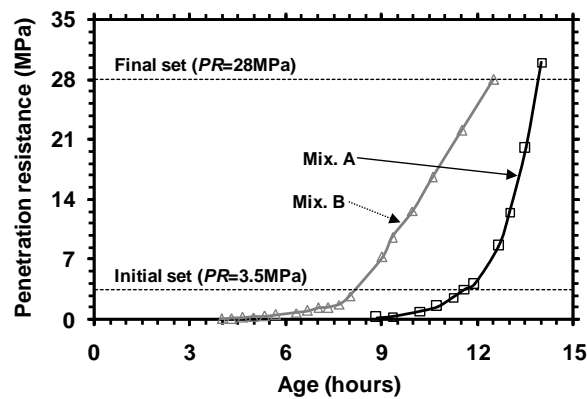


Fig. 6 Penetration resistance versus age

where f_c and f_{ft} are the compressive and flexural strengths of concrete; f_{28} and f_{ft-28} are the compressive and flexural strengths of concrete at 28 days; and, a , b , c , and d are regression constants. The results of nonlinear regression analysis lead to $a=0.971$, $b=-0.271$, $c=0.303$, and $d=-0.058$ for Mix A, and $a=1.162$, $b=-0.326$, $c=0.436$, and $d=-0.101$ for Mix B. The corresponding coefficients of determination (R^2) being larger than 0.97 reveal that exact prediction is possible.

3.2 Setting properties

Fig. 6 presents the setting test results of Mix A and Mix B. The initial and final settings occurred at about 11 h and 13.5 h for Mix A and at about 7.5 h and 11.5 h for Mix B. The faster initial and final setting times measured for Mix B can be explained by the acceleration of the setting provoked by the large quantities of ettringite produced at early age by the introduction of EA in the mixture.

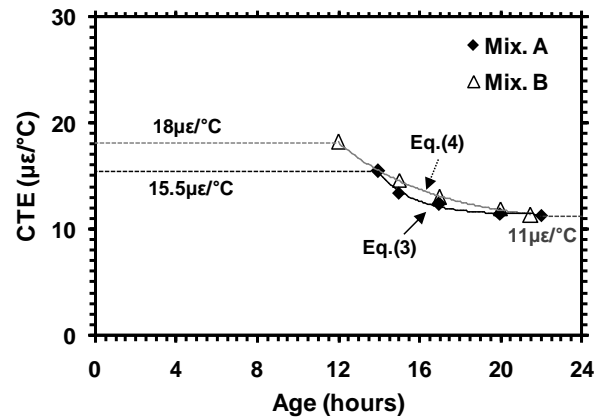


Fig. 7 CTE of UHPC at early age

3.3 Early age CTE of UHPC

Fig. 7 plots the measured CTE of UHPC. As explained above, the measurement of CTE started at the stripping of the mold after final setting. Thus, a constant value corresponding to that at final setting was applied for the CTE prior to final setting. The CTEs of both Mix A and Mix B tended to converge to approximately $11 \mu\epsilon/^\circ\text{C}$ at about 1 day after stripping. Similarly to previous research results, the CTE before hardening of concrete showed extremely high values and exhibited an exponential function-like behavior.

This study proposes prediction formulae for the CTE adopting the form of the equations suggested by Loukili *et al.* (2005). These formulae are expressed in Eqs. (3) and (4) for Mix. A and Mix. B, respectively. Here, the coefficients of determination (R^2) being larger than 0.99 for both Mix A and Mix B reveal that comparatively exact prediction is possible.

$$\text{CTE} = 4.0 \times e^{\frac{14-t}{1.7}} + 11.4 \quad (3)$$

$$\text{CTE} = 7.9 \times e^{\frac{12-t}{4.8}} + 10.3 \quad (4)$$

where CTE ($\mu\epsilon/^\circ\text{C}$) is the coefficient of thermal expansion of concrete; and, t is the age of concrete.

3.4 Autogenous shrinkage of UHPC

Fig. 8 plots the graphs of the variations of the shrinkage strain and internal temperature of the specimens sealed by the aluminum tape. Both mixes showed shrinkage tendency according to the decrease of internal temperature at early age. This was caused by the ambient temperature and is not related to the shrinkage of concrete. In similar with the research of Yoo *et al.* (2013), the deviation point between strain and temperature for UHPC was slightly faster than that of initial set. However, in this study, the time difference between the deviation point and the time of initial set was insignificant and the autogenous shrinkage measured from the deviation point was almost

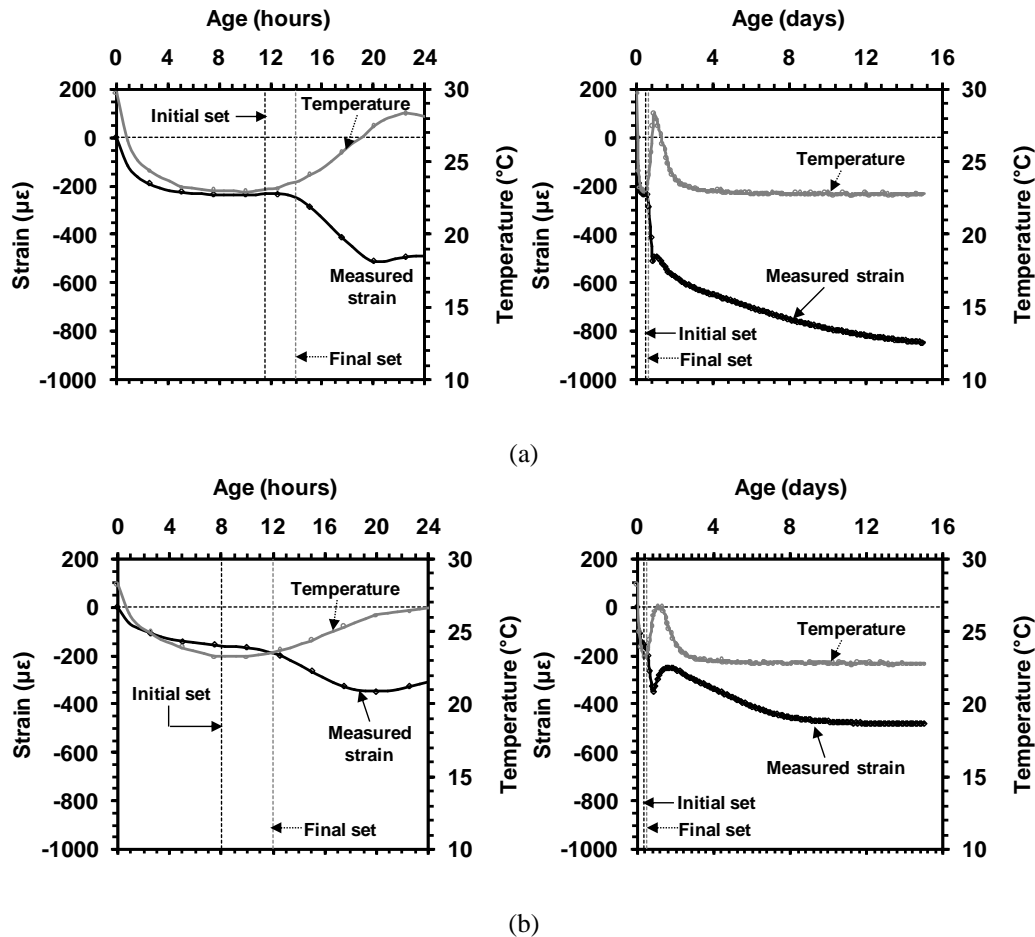


Fig. 8 Measured strain and temperature; (a) Mix. A, (b) Mix. B

same with that measured from initial set. Thus, the initial setting time was used as the zeroing point of autogenous shrinkage measurement according to the JCI recommendation.

In view of the test results, the strain measured with reference to the initial setting time started to exhibit different behavior to the variation of the internal temperature. Mix B experienced volumetric expansion at about 19 h after placing due to the addition of EA in the mix and its shrinkage was seen to have been significantly reduced. The maximum temperature reached approximately 28.4°C and 26.7°C for Mix A and Mix B, respectively.

As can be observed in Fig. 8, a tendency to shrink occurred before initial setting because the temperature of concrete diminished due to the ambient temperature. The sudden increase of shrinkage of Mix. B was about 3 h faster than that of Mix. A. Here, the reason for the faster start of the increase of shrinkage of Mix B compared to Mix A can be attributed to the acceleration of the setting by the admixing of EA (Maltese *et al.* 2005). The sudden decrease of the shrinkage increase rate appeared at approximately 20 h and 18 h for Mix A and Mix B, respectively. This decrease in the shrinkage increase rate was caused by the hardening of concrete, which constrains the volumetric reduction due to the negative pressure in the pores. Mix B exhibited a tendency of

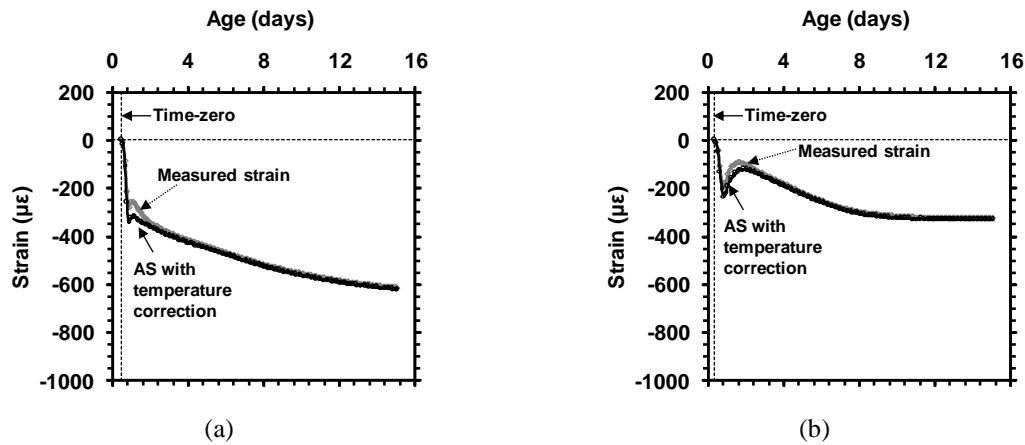


Fig. 9 Comparison of measured strain with autogenous shrinkage; (a) Mix. A, (b) Mix. B

Table 3 Comparison of autogenous shrinkage according to CTE of concrete

	Measured strain ($\mu\epsilon$)		AS with CTE of $11 \mu\epsilon/^\circ\text{C}$ ($\mu\epsilon$)		AS with CTE from Eqs. (3) and (4) ($\mu\epsilon$)	
	At peak temp.	At 15 days	At peak temp.	At 15 days	At peak temp.	At 15 days
Mix. A	-260	-615	-318	-612	-328	-621
Mix. B	-133	-325	-170	-319	-181	-330

Where, AS = autogenous shrinkage

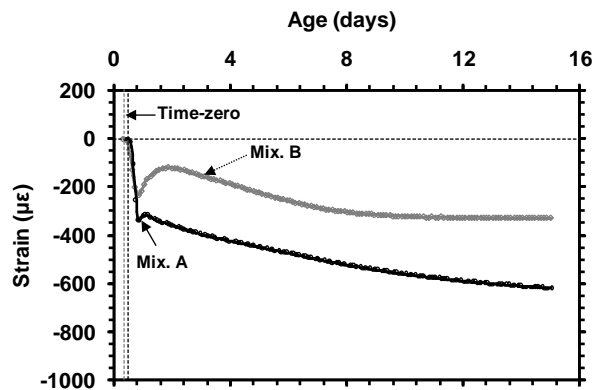


Fig. 10 Autogenous shrinkage with temperature compensation

volumetric expansion since the start of the sudden decrease of the shrinkage increase rate owing to the generation of ettringite by chemical reaction of EA.

Fig. 9 compares the shrinkage strain without temperature compensation and the shrinkage strain in which the measured strain is compensated by considering the CTE. As can be observed, large expansive strain occurred at early age due to the hydration heat of concrete. As listed in Table 3, the autogenous shrinkage considering CTE from Eqs. (3) and (4) was about 26% and 37% higher than the measured strains at peak temperature for Mix. A and Mix. B, respectively. In

contrast, since the temperature increase by hydration heat was relatively small due to the small size of the specimens, the autogenous shrinkage considering a constant CTE of $11 \mu\epsilon/^\circ\text{C}$ was just 3% (for Mix. A) and 6% (for Mix. B) lower than those of the autogenous shrinkage considering CTEs from Eqs. (3) and (4) at peak temperature. The autogenous shrinkage strain in a long-term showed marginal difference according to the temperature compensation, whereas this difference appeared significantly at early age (since the final setting at which hydration heat develops suddenly until the age of 2 days).

Fig. 10 shows the comparison of autogenous shrinkage considering CTEs from Eqs. (3) and (4) of Mix. A and Mix. B. The autogenous shrinkage strain at 15 days for Mix A averaged $-621 \mu\epsilon$. Besides, in the case of Mix B incorporating EA and SRA, the autogenous shrinkage strain at 15 days reached approximately $-330 \mu\epsilon$. Due to the addition of EA and SRA, Mix. B exhibited a large expansion at early age and then it converged to a stable value after nearly 10 days. It is obviously concluded that the use of EA and SRA enables to substantially reduce the autogenous shrinkage by about 47%.

4. Conclusions

This study investigated the mechanical properties of UHPC with respect to the introduction of EA and SRA in the mixture. Autogenous shrinkage test was conducted considering the CTE measured at early age so as to examine the effects of EA and SRA on the autogenous shrinkage behavior of UHPC. The following conclusions can be drawn from this study.

1. The addition of EA and SRA resulted in slight loss of the compressive and flexural strengths at early age. However, the difference in the compressive and flexural strengths caused by the incorporation of EA and SRA became insignificant after 7 days. Moreover, regression constants were suggested based on the prediction formulae for the compressive and flexural strengths of UHPC proposed in a previous study. The predicted values were seen to be in good agreement with the experimental results.

2. The CTEs at early age were obtained by around $15.5 \mu\epsilon/^\circ\text{C}$ and $18 \mu\epsilon/^\circ\text{C}$ for Mix A (mix without EA and SRA) and Mix B (mix with EA and SRA), respectively. In addition, the CTE tended to reduce in the form of an exponential function at further age. The CTE for both Mix A and Mix B appeared to reach approximately $11 \mu\epsilon/^\circ\text{C}$ at 1 day.

3. The combined effect of EA and SRA enabled to reduce the autogenous shrinkage by about 47% at 15 days. When the measured strain was compensated considering the CTE at early age, the shrinkage at peak temperature appeared to be larger by about 26% to 37% than that obtained without compensation. For Mix. B, the point of time at which the autogenous shrinkage started to increase suddenly was about 3 h faster than that of Mix. A. The faster initiation of the sudden increase of the autogenous shrinkage of Mix B could be explained by the acceleration of setting caused by the generation of ettringite at early age owing to the admixing of EA.

Acknowledgements

This research was supported by a grant from a Construction Technology Research Project (Development of impact/blast resistant HPFRCC and evaluation technique thereof (13SCIPS02)) funded by the Ministry on Land, Infrastructure, and Transport.

References

- American Society for Testing and Materials (ASTM) (2006), ASTM C 1609/C 1609M-07 Standard test method for flexural performance of fiber-reinforced concrete (using beam with third point loading), Annual book of ASTM standards, ASTM, West Conshohocken, PA.
- American Society for Testing and Materials (ASTM) (2009), ASTM C 39/C 39M-10 Standard test method for compressive strength of cylindrical concrete specimens, Annual book of ASTM standards, ASTM, West Conshohocken, PA.
- American Society for Testing and Materials (ASTM) (2008), ASTM C 403 Standard test method for time of setting of concrete mixture by penetration resistance, Annual book of ASTM standards, ASTM, West Conshohocken, PA.
- Japan Concrete Institute (1999), *Autogenous Shrinkage of Concrete*, Ed. E. Tazawa, Committee Report, E&FN Spon.
- Kamen, A., Denarie, E., Sadouki, H. and Brühwiler, E. (2008), "Thermo-mechanical response of UHPFRC at early age-Experimental study and numerical simulation", *Cement. Concrete. Res.*, **38**(6), 822-831.
- Kim, S.W., Park, J.J., Kang, S.T., Ryo, G.S. and Koh, K.T. (2008), "Development of ultra high performance cementitious composites (UHPCC) in Korea", *Proceedings of the Fourth International IABMAS Conference*, Seoul, Korea.
- Koh, K.T., Ryu, G.S., Kang, S.T., Park, J.J. and Kim, S.W. (2011), "Shrinkage properties of ultra-high performance concrete (UHPC)", *Adv. Sci. Lett.*, **4**(3), 948-952.
- Loukili, A., Chopin, D., Khelidj, A. and Touzo, J.Y.L. (2000), "A new approach to determine autogenous shrinkage of mortar at an early age considering temperature history", *Cement. Concrete. Res.*, **30**(6), 915-922.
- Maltese, C., Pistolesi, C., Lolli, A., Bravo, A., Cerulli, T. and Salvioni, D. (2005) "Combined effect of expansive and shrinkage reducing admixtures to obtain stable and durable mortars", *Cement. Concrete. Res.*, **35**(12), 2244-2251.
- Park, J.J., Yoo, D.Y., Kim, S.W. and Yoon, Y.S. (2013a), "Drying shrinkage cracking characteristics of ultra-high-performance fibre reinforced concrete with expansive and shrinkage reducing agents", *Mag. Concrete. Res.*, **65**(4), 248-256.
- Park, J.J., Yoo, D.Y., Kim, S.W. and Yoon, Y.S. (2014), "Benefits of using expansive and shrinkage reducing agents in ultra-high-performance concrete for volume stability", *Mag. Concrete. Res.* (In press)
- Yoo, D.Y., Min, K.H., Lee, J.H. and Yoon, Y.S. (2011), "Autogenous shrinkage of concrete with design strength from 60-120N/mm²", *Mag. Concrete. Res.*, **63**(10), 751-761.
- Yoo, D.Y., Park, J.J., Kim, S.W. and Yoon, Y.S. (2013), "Early age setting, shrinkage and tensile characteristics of ultra high performance fiber reinforced concrete", *Constr. Build. Mater.*, **41**(April), 427-438.
- Yoo, D.Y., Park, J.J., Kim, S.W. and Yoon, Y.S. (2014), "Influence of reinforcing bar type on autogenous shrinkage stress and bond behavior of ultra high performance fiber reinforced concrete", *Cement. Concrete. Comp.* (In press)